



An adaptive splitting approach for the quenching solution of reaction–diffusion equations over nonuniform grids

Matthew A. Beauregard^{*}, Qin Sheng

Department of Mathematics and Center for Astrophysics, Space Physics and Engineering Research, Baylor University, One Bear Place # 97328, Waco, TX 76798, United States

ARTICLE INFO

Article history:

Received 26 April 2011

Received in revised form 2 October 2012

Keywords:

Reaction–diffusion equations

Quenching singularity

Degeneracy

Splitting method

Adaptation

Nonuniform grids

ABSTRACT

The numerical solution of a nonlinear degenerate reaction–diffusion equation of the quenching type is investigated. While spatial derivatives are discretized over symmetric nonuniform meshes, a Peaceman–Rachford splitting method is employed to advance solutions of the semidiscretized system. The temporal step is determined adaptively through a suitable arc-length monitor function. A criterion is derived to ensure that the numerical solution acquired preserves correctly the positivity and monotonicity of the analytical solution. Weak stability is proven in a von Neumann sense via the ∞ -norm. Computational examples are presented to illustrate our results.

© 2012 Elsevier B.V. All rights reserved.

1. Introduction

Nonlinear degenerate reaction–diffusion equations of the quenching type play a vital role in modeling many important physical and engineering processes such as with the modeling of internal combustion [1–4]. These mathematical models may develop singularities in solutions or their derivatives in finite time [2,5–7]. The phenomena can be physically observed when certain environmental parameters exceed their limits in applications. A mathematical interpretation of such singularities is that the nonlinear forcing terms in the differential equations become unbounded when certain critical values are reached in finite time [2,8–10,7]. It has been extremely meaningful to estimate these critical values and the time upon which a quenching may occur through efficient and effective numerical algorithms [6,11–13].

Consider a two-dimensional solid fuel ignition model where the activation energy method has decoupled, that is, the dynamics of temperature is independent of the single-species mass fraction [14]. Let $D = (0, a) \times (0, b)$ for $a, b > 0$, ∂D be its boundary, and let $\Omega = D \times (0, T)$, $S = \partial D \times (0, T)$ where $T \in (0, \infty)$. A degenerate reaction–diffusion problem of the quenching type modeling the anticipated internal combustion process is [5,9,10]

$$(x^2 + y^2)^{q/2} u_t = u_{xx} + u_{yy} + f(u), \quad q \geq 0, (x, y, t) \in \Omega, \quad (1.1)$$

$$u(x, y, t) = 0, \quad (x, y, t) \in S, \quad (1.2)$$

$$u(x, y, 0) = u_0(x, y), \quad (x, y) \in D, \quad (1.3)$$

where the nonlinear source function, $f(u)$, is strictly increasing for $0 \leq u < 1$ with

$$f(0) = f_0 > 0, \quad \lim_{u \rightarrow 1^-} f(u) = \infty.$$

^{*} Corresponding author.

E-mail address: Matthew_Beauregard@baylor.edu (M.A. Beauregard).

The function $u(x, y, t)$ represents the temperature in the rectangular channel, and x and y are coordinates in the perpendicular and parallel directions to the channel walls, respectively. The function $(x^2 + y^2)^{q/2}$ represents a singularity in the temperature transportation speed causing a degeneracy in Eq. (1.1) [2,15,16]. The parameter $q \in [0, 2)$, for which values close to two indicate a stronger degeneracy in the modeling equation, that is, a stronger defect in the transportation of heat throughout the channel, thus breaking symmetry. The upper bound on q ensures that the inverse of the degeneracy is integrable in the $L^2(D)$ space. The initial temperature $0 \leq u_0 \ll 1$. The solution of (1.1)–(1.3) is said to *quench* if there exists a finite time T_c such that

$$\sup \{|u_t(x, y, t)| : (x, y) \in \bar{D}\} \rightarrow \infty, \quad \text{as } t \rightarrow T_c^-. \quad (1.4)$$

The value of T_c is referred as the *quenching time*. A necessary condition for this to occur is

$$\max \{|u(x, y, t)| : (x, y) \in \bar{D}\} \rightarrow 1^-, \quad \text{as } t \rightarrow T_c^-. \quad (1.5)$$

It has been shown that if f, f_u are nonnegative, then, for any fixed ratio a/b , there exists a unique critical domain D_c , the *quenching domain*, for which the solution of (1.1)–(1.3) quenches and is unique prior to T_c [17,18,9].

Although considerable efforts have been devoted to the field in recent years [5,19,20,10,11,21,22], the development of the theory and computation of quenching solutions, including estimations of quenching domains for (1.1)–(1.3), is still in its infancy. The complication in the numerical study is owed primarily to the following two facts. First, the strong nonlinear singularity may cause rapid changes in the gradient and time derivatives of u as quenching is approached. This requires fine resolution in the spatial and temporal grids. Adaptation of the underlying grids in space and time are often necessary for capturing the singularity precisely. Second, quenching type models are often multi-dimensional and attention needs to be given to the efficiently in singular computations. Splitting techniques have an edge on this issue as they offer efficient and effective means of advancing the numerical solution despite the Sheng–Suzuki barrier [23].

Motivated by aforementioned concerns, this paper focuses on a highly efficient algorithm that employs temporal adaptation coupled with nonuniform meshes. In particular, a suitable criterion is derived that preserves both positive and monotonic properties of the numerical solution while a weak stability is maintained in the presence of perturbations. Additionally, we motivate the use of specially-tailored exponentially graded grids, that is, static nonuniform grids focused about the quenching location. These grids are developed from a priori knowledge of the quenching location and solution shape. Our computational experiments indicate that the employment of such grids allow the computation to be accomplished with fewer grid points while maintaining an excellent agreement with prior results that used larger fixed, fine, and uniform meshes [5,10].

This paper is organized as follows. In Section 2, a second order Peaceman–Rachford splitting scheme is introduced for solving the singular problem (1.1)–(1.3) directly. Temporal steps are determined adaptively through a suitable arc-length monitor function [5]. Finite differences for approximating the spatial derivatives are introduced over a symmetric nonuniform mesh. In Section 3, it is shown that the monotonic property is conserved by the sequence of discrete solutions. Section 4 is devoted to a study of the numerical stability of the adaptive splitting method implemented. Further, Section 5 provides two illustrative examples from computational experiments calculating quenching domains and respective quenching times with the proposed decomposition algorithm. It is found that our results match existing calculations and theoretical predictions satisfactorily. Moreover, the agreement between the theoretical and numerical predictions are improved. Finally, a brief summary about the results obtained, as well as some concerns and expectations, are given in Section 6. In the ensuing discussion all lowercase bold letters indicate vectors, uppercase letters are used for matrices. The infinity-norm is used throughout discussions unless otherwise specified.

2. Variable step splitting scheme

The problem (1.1)–(1.3) is rescaled, namely,

$$\begin{aligned} u_t &= \frac{1}{a^2\phi(x, y)}u_{xx} + \frac{1}{b^2\phi(x, y)}u_{yy} + \frac{f(u)}{\phi(x, y)}, \quad (x, y, t) \in \Omega, \\ 0 &= u(0, y, t) = u(1, y, t) = u(x, 0, t) = u(x, 1, t), \quad (x, y, t) \in S, \\ u(x, y, 0) &= u_0(x, y), \quad (x, y) \in D, \end{aligned}$$

where $\phi(x, y) = (a^2x^2 + b^2y^2)^{q/2}$, $q \geq 0$, and $D = (0, 1) \times (0, 1)$.

Utilizing the nonuniform central difference approximation formulas discussed in [24], for given $N > 1$, we may replace spatial derivatives in the differential equation on any variable step mesh (x_i, y_j) , for $i, j = 0, \dots, N$. Let $h_k = x_{k+1} - x_k = y_{k+1} - y_k$ be the spatial step-size in both x and y directions. Consider a set of nonuniform step-sizes defined by

$$h_k = \frac{1}{2\sqrt{N^*}} \left[\sqrt{N^* + \frac{1}{2} - \left| k - \left(N^* - \frac{1}{2} \right) \right|} - \sqrt{N^* - \frac{1}{2} - \left| k - \left(N^* - \frac{1}{2} \right) \right|} \right], \quad (2.1)$$

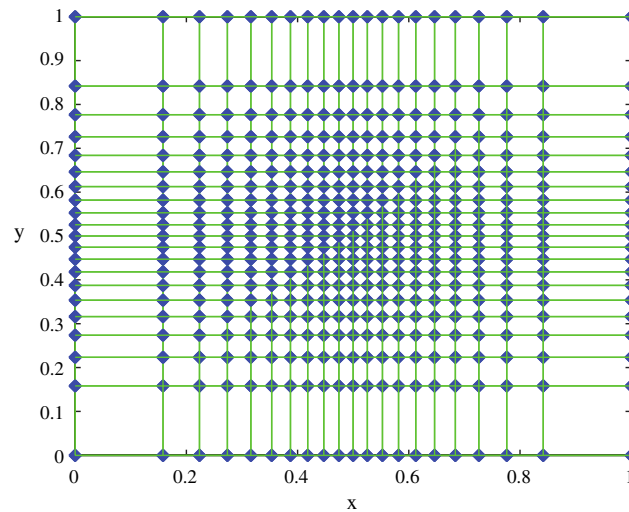


Fig. 1. An illustration of a typical symmetric nonuniform mesh calculated from (2.1). For quenching problems a graded mesh is often computationally efficient as it follows the blow-up pattern of the time-derivative closely.

for $k = 0, \dots, 2N^* - 1 = N$. Based on the above set, a typical two-dimensional symmetric mesh is illustrated in Fig. 1. Note that, although the center of this graded mesh is not exactly the quenching point due to the degeneracy [5,7], the ensuing computations based on it can be quite effective and efficient.

Let $u_{i,j}(t)$ be an approximation of the solution at (x_i, y_j, t) . The semidiscretized equations based on (1.1) are

$$\begin{aligned} \dot{u}_{i,j} = & \frac{1}{a^2 \phi(x_i, y_j)} \left(\frac{2}{h_{i-1}(h_{i-1} + h_i)} u_{i-1,j} - \frac{2}{h_i h_{i-1}} u_{i,j} + \frac{2}{h_i(h_{i-1} + h_i)} u_{i+1,j} \right) \\ & + \frac{1}{b^2 \phi(x_i, y_j)} \left(\frac{2}{h_{j-1}(h_{j-1} + h_j)} u_{i,j-1} - \frac{2}{h_j h_{j-1}} u_{i,j} + \frac{2}{h_j(h_{j-1} + h_j)} u_{i,j+1} \right) + \frac{f(u_{i,j})}{\phi(x_i, y_j)}, \end{aligned}$$

where

$$\phi(x_i, y_j) = \left[a^2 \left(\sum_{k=0}^{i-1} h_k \right)^2 + b^2 \left(\sum_{k=0}^{j-1} h_k \right)^2 \right]^{q/2}.$$

Denote $\mathbf{v}(t) = (u_{1,1}, u_{2,1}, \dots, u_{N,1}, u_{1,2}, \dots, u_{N,N})^\top$. The semidiscretized system corresponding to (1.1)–(1.3) can be written compactly as

$$\dot{\mathbf{v}} = P\mathbf{v} + R\mathbf{v} + \mathbf{g}(\mathbf{v}), \quad (2.2)$$

$$\mathbf{g} = \left(\frac{f(u_{1,1})}{\phi(x_1, y_1)}, \dots, \frac{f(u_{N,N})}{\phi(x_N, y_N)} \right)^\top, \quad (2.3)$$

$$\mathbf{v}(0) = \mathbf{v}_0, \quad (2.4)$$

where P and R are $N^2 \times N^2$ matrices, namely,

$$P = \frac{1}{a^2} B(I_N \otimes T), \quad R = \frac{1}{b^2} B(T \otimes I_N),$$

where I_N is the $N \times N$ identity matrix and \otimes denotes the Kronecker product. Further, T is a tridiagonal matrix with upper, main, and lower diagonals of the form

$$\begin{aligned} u_i &= \frac{2}{h_i(h_i + h_{i-1})}, & l_i &= \frac{2}{h_i(h_{i+1} + h_i)}, & i &= 1, \dots, N-1, \\ m_i &= -\frac{2}{h_i h_{i-1}}, & i &= 1, \dots, N. \end{aligned}$$

It is observed that in general T is not symmetric unless $h_{i-1} = h_{i+1}$. However it is not difficult to show that T is similar to a symmetric matrix. In addition, it is always diagonally dominant by rows. The matrix P is block diagonal with tridiagonal blocks while R is block tridiagonal with diagonal blocks.

On the other hand, the matrix B is diagonal with diagonal blocks $B^{(j)} = \text{diag}(\psi_{ij}^{-1})$, where $\psi_{ij}^{-1} = \phi(x_i, y_j)^{-1}$ for $i, j = 1, \dots, N$.

The formal solution of Eqs. (2.2)–(2.4) is

$$\mathbf{v}(t) = e^{tC} \mathbf{v}_0 + \int_0^t e^{(t-\tau)C} \mathbf{g}(\mathbf{v}(\tau)) d\tau, \quad (2.5)$$

where $C = P + R$. A trapezoidal rule can be utilized to approximate the integral with a second-order accuracy,

$$\mathbf{v}(t) = e^{tC} \mathbf{v}_0 + \frac{t}{2} (\mathbf{g}(\mathbf{v}(t)) + e^{tC} \mathbf{g}(\mathbf{v}_0)) + O(t^2). \quad (2.6)$$

On the other hand, consider the Peaceman–Rachford splitting formula [5,21],

$$e^{tC} = p(t) + O(t^2), \quad (2.7)$$

where

$$p(t) = \left(I - \frac{t}{2}R\right)^{-1} \left(I - \frac{t}{2}P\right)^{-1} \left(I + \frac{t}{2}P\right) \left(I + \frac{t}{2}R\right).$$

From Eqs. (2.6) and (2.7) we arrive at the following variable time step Peaceman–Rachford splitting scheme,

$$\mathbf{v}_{k+1} = \left(I - \frac{\tau_k}{2}R\right)^{-1} \left(I - \frac{\tau_k}{2}P\right)^{-1} \left(I + \frac{\tau_k}{2}P\right) \left(I + \frac{\tau_k}{2}R\right) \left(\mathbf{v}_k + \frac{\tau_k}{2} \mathbf{g}(\mathbf{v}_k)\right) + \frac{\tau_k}{2} \mathbf{g}(\mathbf{w}^{(k)}) + O(\tau_k^2), \quad (2.8)$$

where τ_k is the variable time step and $\mathbf{w}^{(k)}$ is a suitable approximation to \mathbf{v}_{k+1} . For instance, using a right sum quadrature in Eq. (2.5) and neglecting second order terms results in $\mathbf{w}^{(k)} = \mathbf{v}_k + \tau_k (C\mathbf{v}_k + \mathbf{g}(\mathbf{v}_k))$.

Prior to quenching the time derivative will need to be resolved at finer time steps. In light of Eqs. (1.4) and (1.5), an arc-length monitor function for \mathbf{v}_t can be introduced. A typical choice is

$$m_i \left(\frac{\partial v_i}{\partial t}, t \right) = \sqrt{1 + \left(\frac{\partial^2 v_i}{\partial t^2} \right)^2}, \quad (x, y, t) \in \Omega, \quad (2.9)$$

and for $i = 1, \dots, N^2$. The maximal arc-lengths in neighboring intervals $[t_{k-2}, t_{k-1}]$ and $[t_{k-1}, t_k]$ are chosen to be equivalent resulting in an equation for τ_k for each i . The new temporal step is then taken as the minimum over all i , namely,

$$\tau_k^2 = \tau_{k-1}^2 + \min_i \left\{ \left[\left(\frac{\partial v_i}{\partial t} \right)_{k-1} - \left(\frac{\partial v_i}{\partial t} \right)_{k-2} \right]^2 - \left[\left(\frac{\partial v_i}{\partial t} \right)_k - \left(\frac{\partial v_i}{\partial t} \right)_{k-1} \right]^2 \right\}, \quad k = 2, \dots,$$

with τ_0 and τ_1 given.

3. Monotonic property

It is well-known that the positivity and monotonicity are of fundamental importance to quenching solutions of nonlinear reaction–diffusion equations of the quenching type, such as Eqs. (1.1)–(1.3) [1,17,6,9]. These properties arise out of the physical model that the underlying equations are representing [14,6,3,16]. It is therefore of the utmost importance to exhibit these key qualities in the discrete case.

Lemma 3.1. $\|T\| \leq \max_{i=1,\dots,N} \left\{ \frac{6}{h_i h_{i-1}} \right\}$.

Proof. Consider the infinity norm of T , namely,

$$\|T\| = \max \left\{ u_1 - m_1, l_{N-1} - m_N, \max_{i=1,\dots,N} \{l_{i-1} + u_i - m_i\} \right\} \leq 3 \max_{i=1,\dots,N} |m_i|. \quad \square$$

Lemma 3.2. If

$$\frac{\tau_k}{\beta_{\min}} < \min \{a^2, b^2\},$$

where

$$\beta_{\min} = \frac{1}{3} \|B\|^{-1} \min_{i=1,\dots,N} \{h_i h_{i-1}\},$$

$$\|B\|^{-1} = \psi_{\min} = h_0^q (a^2 + b^2)^{q/2},$$

then the matrices

$$I - \frac{\tau_k}{2}P, \quad I - \frac{\tau_k}{2}R, \quad I + \frac{\tau_k}{2}P, \quad \text{and} \quad I + \frac{\tau_k}{2}R$$

are nonsingular. Also, $I - \frac{\tau_k}{2}P$ and $I - \frac{\tau_k}{2}R$ are monotone and inverse positive. $I + \frac{\tau_k}{2}P$ and $I + \frac{\tau_k}{2}R$ are nonnegative. Similarly, if $\frac{\tau_k}{\beta_{\min}} < \frac{1}{4} \min \{a^2, b^2\}$, then $I + \tau_k C$ is nonsingular as well as nonnegative where $C = P + R$.

Proof. By Lemma 3.1 the norm of $\frac{\tau_k}{2}P$ must be bounded, that is,

$$\begin{aligned} \left\| \frac{\tau_k}{2}P \right\| &= \frac{\tau_k}{2a^2} \|B(I_N \otimes T)\| \\ &\leq \frac{\tau_k}{2a^2} \|B\| \|I_N \otimes T\| = \frac{\tau_k}{2a^2} \|B\| \|T\| \\ &\leq \frac{\tau_k}{a^2} \|B\| \max_i \left\{ \frac{3}{h_i h_{i-1}} \right\} < 1. \end{aligned}$$

Hence $I + \frac{\tau_k}{2}P$ is nonsingular [25]. Clearly it is also nonnegative. A similar argument shows that $I + \frac{\tau_k}{2}R$ is nonsingular and nonnegative. In addition, if $\frac{\tau_k}{\beta_{\min}} < \frac{1}{4} \min \{a^2, b^2\}$ then

$$\begin{aligned} \|\tau_k(P + R)\| &\leq \tau_k \|P\| + \tau_k \|R\| \\ &\leq \tau_k \left(\frac{1}{a^2} + \frac{1}{b^2} \right) \left(\frac{2}{\frac{1}{3}h_0^q (a^2 + b^2)^{q/2} \min_i \{h_i h_{i-1}\}} \right) < 1. \end{aligned}$$

Hence $I + \tau_k(P + R)$ is nonsingular and clearly nonnegative.

Consider the matrix $M = I - \frac{\tau_k}{2}P$. As $M_{ij} \leq 0$ for $i \neq j$ and the weak row sum criterion is satisfied M is monotone and hence an inverse exists for which is nonnegative [25]. The matrix $I - \frac{\tau_k}{2}P$ is also inverse-positive. Using a similar argument shows that $I - \frac{\tau_k}{2}R$ is inverse-positive. \square

Remark 3.1. It is observed that the criterion on the temporal step for a uniform mesh is a third smaller than that shown in [5]. This is a result of using the infinity norm rather than the ℓ^2 -norm. Furthermore, if the ℓ^2 -norm is considered with the same criterion on τ_k , a similar proof of the lemma is accomplished by using the standard inequality $\|A\|_2^2 \leq \|A\|_1 \|A\|_\infty$.

Remark 3.2. It is clear that the criterion on τ_k is attributed to the choice of the norm used. For instance the $\frac{1}{3}$ factor can easily be removed if the entry-wise maximum-norm is considered. However, that norm is highly undesirable owing to the fact that it is not sub-multiplicative, a property that needs to be exploited in the ensuing stability analysis.

The next lemma shows that for a uniform time step the numerical solution monotonically increases.

Lemma 3.3. Let $C\mathbf{v}_\ell + \mathbf{g}(\mathbf{v}_\ell) + \frac{\tau_\ell^2}{4}PR\mathbf{g}(\mathbf{v}_\ell) > 0$, where $\ell \geq 0$ is any beginning time step. If

- (i) $\tau_k = \tau_\ell$ for all $k \geq \ell$,
- (ii) $\frac{\tau_k}{\beta_{\min}} < \frac{1}{4} \min \{a^2, b^2\}$,

then $\mathbf{v}_{k+1} > \mathbf{v}_k$ for all $k \geq \ell$. The sequence $\{\mathbf{v}_k\}_{k=\ell}^\infty$ is therefore monotonically increasing.

Proof. The proof is identical to that found in [5] where the nonnegativity of C is guaranteed by assumption (ii) and using Lemma 3.2. \square

Remark 3.3. The previous lemmas can all easily be modified for the case of a non-symmetric mesh in x and y and each follow a similar proof as described above.

In the following lemma it will be shown that for the initial time step (ii) in Lemma 3.3 is satisfied.

Lemma 3.4. If $\mathbf{v}_0 = 0$ and $\frac{\tau_0}{\beta_{\min}} < \min \{a^2, b^2\}$ then $C\mathbf{v}_0 + \mathbf{g}(\mathbf{v}_0) + \frac{\tau_0^2}{4}PR\mathbf{g}(\mathbf{v}_0) > 0$.

Proof. Let $\mathbf{v}_0 = 0$ then

$$f_0\boldsymbol{\Psi} := \mathbf{g}(0) + \frac{\tau_0^2}{4}PR\mathbf{g}(0) = f_0 \left(I + \frac{\tau_0^2}{4}PR \right) \boldsymbol{\xi},$$

where $f_0 > 0$, $\xi = \left(\frac{1}{\psi_{1,1}}, \frac{1}{\psi_{2,1}}, \dots, \frac{1}{\psi_{N,N}}\right)^\top$, and $\Psi = (\psi_{1,1}, \psi_{2,1}, \dots, \psi_{N,N})^\top$. Clearly all the components of $\xi > 0$. Consider $\psi_{m,n}$ for $m, n = 2, \dots, N-1$,

$$\begin{aligned} \psi_{m,n} = \psi_{m,n}^{-1} & \left\{ 1 + \frac{\tau_0^2}{a^2 b^2} \left[\psi_{m-1,n}^{-1} \psi_{m-1,n-1}^{-1} \frac{1}{h_{m-1}(h_m + h_{m-1})h_{n-1}(h_n + h_{n-1})} \right. \right. \\ & - \psi_{m,n}^{-1} \psi_{m,n-1}^{-1} \frac{1}{h_m h_{m-1} h_{n-1}(h_n + h_{n-1})} + \psi_{m+1,n}^{-1} \psi_{m+1,n-1}^{-1} \frac{1}{h_m(h_m + h_{m-1})h_{n-1}(h_n + h_{n-1})} \\ & - \psi_{m-1,n}^{-1} \psi_{m-1,n}^{-1} \frac{1}{h_{m-1}(h_m + h_{m-1})h_n h_{n-1}} + \psi_{m,n}^{-1} \psi_{m,n}^{-1} \frac{1}{h_m h_{m-1} h_n h_{n-1}} \\ & - \psi_{m+1,n}^{-1} \psi_{m+1,n}^{-1} \frac{1}{h_m(h_m + h_{m-1})h_n h_{n-1}} + \psi_{m-1,n}^{-1} \psi_{m-1,n+1}^{-1} \frac{1}{h_{m-1}(h_m + h_{m-1})h_n(h_n + h_{n-1})} \\ & \left. \left. - \psi_{m,n}^{-1} \psi_{m,n+1}^{-1} \frac{1}{h_m h_{m-1} h_n(h_n + h_{n-1})} + \psi_{m+1,n}^{-1} \psi_{m+1,n+1}^{-1} \frac{1}{h_m(h_m + h_{m-1})h_n(h_n + h_{n-1})} \right] \right\}. \end{aligned}$$

Recall that $\psi_{1,1}^{-1} \geq \psi_{m,n}^{-1}$. It can be readily verified that

$$\frac{\tau_0^2 \psi_{1,1}^{-2}}{a^2 b^2} < \frac{1}{3} \min_i \{h_i h_{i-1}\}^2.$$

It follows therefore

$$\psi_{m,n} \geq \psi_{m,n}^{-1} \left\{ 1 - \frac{\tau_0^2 \psi_{1,1}^{-2}}{a^2 b^2} \left[\frac{3}{\min_i \{h_i h_{i-1}\}^2} \right] \right\} > 0.$$

Now, consider functions $\psi_{1,n}$, where $n = 2, \dots, N-1$,

$$\begin{aligned} \psi_{1,n} = \psi_{1,n}^{-1} & \left\{ 1 + \frac{\tau_0^2}{a^2 b^2} \left[-\psi_{1,n}^{-1} \psi_{1,n-1}^{-1} \frac{1}{h_1 h_0 h_{n-1}(h_n + h_{n-1})} + \psi_{2,n}^{-1} \psi_{2,n-1}^{-1} \frac{1}{h_1(h_1 + h_0)h_{n-1}(h_n + h_{n-1})} \right. \right. \\ & + \psi_{1,n}^{-1} \psi_{1,n}^{-1} \frac{1}{h_1 h_0 h_n h_{n-1}} - \psi_{2,n}^{-1} \psi_{2,n}^{-1} \frac{1}{h_1(h_1 + h_0)h_n h_{n-1}} - \psi_{1,n}^{-1} \psi_{1,n+1}^{-1} \frac{1}{h_1 h_0 h_n(h_n + h_{n-1})} \\ & \left. \left. + \psi_{2,n}^{-1} \psi_{2,n+1}^{-1} \frac{1}{h_1(h_1 + h_0)h_n(h_n + h_{n-1})} \right] \right\} \\ & \geq \psi_{1,n}^{-1} \left\{ 1 - \frac{\tau_0^2 \psi_{1,1}^{-2}}{a^2 b^2} \left[\frac{2}{\min_i \{h_i h_{i-1}\}^2} \right] \right\} > 0. \end{aligned}$$

Similarly for $m = N$ and $n = 2, \dots, N-1$,

$$\begin{aligned} \psi_{N,n} = \psi_{N,n}^{-1} & \left\{ 1 + \frac{\tau_0^2}{a^2 b^2} \left[\psi_{N-1,n}^{-1} \psi_{N-1,n-1}^{-1} \frac{1}{h_{N-1}(h_N + h_{N-1})h_{n-1}(h_n + h_{n-1})} \right. \right. \\ & - \psi_{N,n}^{-1} \psi_{N,n-1}^{-1} \frac{1}{h_N h_{N-1} h_{n-1}(h_n + h_{n-1})} \\ & - \psi_{N-1,n}^{-1} \psi_{N-1,n}^{-1} \frac{1}{h_{N-1}(h_N + h_{N-1})h_n h_{n-1}} + \psi_{N,n}^{-1} \psi_{N,n}^{-1} \frac{1}{h_N h_{N-1} h_n h_{n-1}} \\ & \left. \left. + \psi_{N-1,n}^{-1} \psi_{N-1,n+1}^{-1} \frac{1}{h_{N-1}(h_N + h_{N-1})h_n(h_n + h_{n-1})} - \psi_{N,n}^{-1} \psi_{N,n+1}^{-1} \frac{1}{h_N h_{N-1} h_n(h_n + h_{n-1})} \right] \right\} \\ & \geq \psi_{N,n}^{-1} \left\{ 1 - \frac{\tau_0^2 \psi_{1,1}^{-2}}{a^2 b^2} \left[\frac{2}{\min_i \{h_i h_{i-1}\}^2} \right] \right\} > 0. \end{aligned}$$

The remaining six cases follow a similar proof and can be shown to be strictly greater than zero. \square

Lemma 3.5. If $\frac{\tau}{\beta_{\min}} < \min\{a^2, b^2\}$ then the components of

$$\mathbf{w} = \left(-C \pm \frac{\tau}{2} PR\right) \mathbf{x} \geq 0,$$

where $\mathbf{x} = (1, 1, \dots, 1)^\top$.

Proof. Let the vector $\mathbf{w} = (w_{1,1}, w_{2,1}, \dots, w_{m,n}, \dots, w_{N,N})^\top$. For $m, n = 2, \dots, N-1$,

$$w_{m,n} = \pm \frac{2\tau\psi_{m,n}^{-1}}{a^2b^2} \left(\frac{\psi_{m-1,n}^{-1}}{h_{m-1}(h_m + h_{m-1})} - \frac{\psi_{m,n}^{-1}}{h_m h_{m-1}} + \frac{\psi_{m+1,n}^{-1}}{h_m(h_m + h_{m-1})} \right) \\ \times \left(\frac{1}{h_{n-1}(h_n + h_{n-1})} - \frac{1}{h_n h_{n-1}} + \frac{1}{h_n(h_n + h_{n-1})} \right) = 0.$$

Consider $w_{1,n}$ where $n = 2, \dots, N-1$,

$$w_{1,n} = \frac{2\psi_{1,n}^{-1}}{a^2} \left(\frac{1}{h_1 h_0} - \frac{1}{h_0(h_1 + h_0)} \right) > 0.$$

Similarly,

$$w_{N,n} = \frac{2\psi_{N,n}^{-1}}{a^2} \left(\frac{1}{h_N h_{N-1}} - \frac{1}{h_{N-1}(h_N + h_{N-1})} \right) > 0.$$

Now consider $w_{m,1}$ for $m = 2, \dots, N-1$. Then

$$w_{m,1} = \frac{2\psi_{m,1}^{-1}}{b^2} \left(\frac{1}{h_1 h_0} - \frac{1}{h_1(h_1 + h_0)} \right) \left[1 \mp \frac{2\tau}{a^2} \left(\frac{\psi_{m-1,1}^{-1}}{h_{m-1}(h_m + h_{m-1})} - \frac{\psi_{m,1}^{-1}}{h_m h_{m-1}} + \frac{\psi_{m+1,1}^{-1}}{h_m(h_m + h_{m-1})} \right) \right] \\ \geq \frac{2\psi_{m,1}^{-1}}{b^2} \left(\frac{1}{h_1 h_0} - \frac{1}{h_1(h_1 + h_0)} \right) \left[1 - \frac{2\tau}{a^2} \left(\frac{\psi_{\min}^{-1}}{\min_i \{h_i h_{i-1}\}} \right) \right] > 0.$$

Lastly,

$$w_{m,N} = \frac{2\psi_{m,N}^{-1}}{b^2} \left(\frac{1}{h_N h_{N-1}} - \frac{1}{h_{N-1}(h_N + h_{N-1})} \right) \left[1 \mp \frac{2\tau}{a^2} \left(\frac{\psi_{m-1,N}^{-1}}{h_{m-1}(h_m + h_{m-1})} - \frac{\psi_{m,N}^{-1}}{h_m h_{m-1}} + \frac{\psi_{m+1,N}^{-1}}{h_m(h_m + h_{m-1})} \right) \right] \\ \geq \frac{2\psi_{m,N}^{-1}}{b^2} \left(\frac{1}{h_N h_{N-1}} - \frac{1}{h_{N-1}(h_N + h_{N-1})} \right) \left[1 - \frac{2\tau}{a^2} \left(\frac{\psi_{\min}^{-1}}{\min_i \{h_i h_{i-1}\}} \right) \right] > 0.$$

The remaining cases for $m = 1$ and N follow identical proofs. \square

It is clear that with a uniform time step the numerical solution is guaranteed to monotonically increase. Moreover the following lemma will show that in the first time step the solution will not quench.

Lemma 3.6. *If*

$$\frac{\tau_0}{\beta_{\min}} < \min \{a^2, b^2\}$$

and

$$\min_i \{h_i h_{i-1}\} < \frac{3}{4M \min \{a^2, b^2\}},$$

where

$$M = f(\tau_0 f_0 \psi_{\min}^{-1}),$$

then given $\mathbf{v}_0 = 0$ all the components of $\mathbf{v}_1 < 1$.

Proof. By Eq. (2.8) we have

$$\mathbf{v}_1 = \left(I - \frac{\tau_0}{2} R \right)^{-1} \left(I - \frac{\tau_0}{2} P \right)^{-1} \left(I + \frac{\tau_0}{2} P \right) \left(I + \frac{\tau_0}{2} R \right) \frac{\tau_0}{2} f_0 \xi + \frac{\tau_0}{2} \mathbf{g}(\tau_0 f_0 \xi),$$

where $\mathbf{g}(\mathbf{w}^0) = \mathbf{g}(\mathbf{v}_0 + \tau_0(C\mathbf{v}_0 + \mathbf{g}(\mathbf{v}_0))) = \mathbf{g}(\tau_0 f_0 \xi)$ has been utilized. Clearly $\mathbf{g}(\tau_0 \mathbf{g}(0)) \leq M\xi$ and $f_0 \leq M$ as $f(u)$ monotonically increases. Let $\mathbf{x} = (1, 1, \dots, 1)^\top$. Consider the difference

$$\mathbf{v}_1 - \mathbf{x} = \left(I - \frac{\tau_0}{2} R \right)^{-1} \left(I - \frac{\tau_0}{2} P \right)^{-1} \left[\frac{\tau_0}{2} \left(I + \frac{\tau_0}{2} P \right) \left(I + \frac{\tau_0}{2} R \right) f_0 \xi \right. \\ \left. + \frac{\tau_0}{2} \left(I - \frac{\tau_0}{2} P \right) \left(I - \frac{\tau_0}{2} R \right) \mathbf{g}(\tau_0 f_0 \xi) - \left(I - \frac{\tau_0}{2} P \right) \left(I - \frac{\tau_0}{2} R \right) \mathbf{x} \right]$$

$$\begin{aligned}
&\leq \left(I - \frac{\tau_0}{2}R\right)^{-1} \left(I - \frac{\tau_0}{2}P\right)^{-1} \left[\frac{\tau_0}{2} \left(I + \frac{\tau_0}{2}P\right) \left(I + \frac{\tau_0}{2}R\right) f_0 \xi \right. \\
&\quad \left. + \frac{\tau_0}{2} \left(I - \frac{\tau_0}{2}P\right) \left(I - \frac{\tau_0}{2}R\right) M \xi - \left(I - \frac{\tau_0}{2}P\right) \left(I - \frac{\tau_0}{2}R\right) \mathbf{x} \right] \\
&= \left(I - \frac{\tau_0}{2}R\right)^{-1} \left(I - \frac{\tau_0}{2}P\right)^{-1} \mathbf{s}.
\end{aligned}$$

Since $\tau_0/\beta_{\min} < \min\{a^2, b^2\}$ then $(I - \frac{\tau_k}{2}R)^{-1}$ and $(I - \frac{\tau_k}{2}P)^{-1}$ are nonnegative by Lemma 3.2. All of the components of \mathbf{s} will be shown to be less than zero, which will complete the proof. Consider the absolute value of the first two terms of \mathbf{s} , using the fact that both $I + \frac{\tau_0}{2}P$ and $I + \frac{\tau_0}{2}R$ are nonnegative,

$$\begin{aligned}
|\mathbf{s}^+| &= \left| \frac{\tau_0}{2} \left(I + \frac{\tau_0}{2}P\right) \left(I + \frac{\tau_0}{2}R\right) f_0 \xi + \frac{\tau_0}{2} \left(I - \frac{\tau_0}{2}P\right) \left(I - \frac{\tau_0}{2}R\right) M \xi \right| \\
&\leq \tau_0 M \psi_{\min}^{-1} \left\| \left(I + \frac{\tau_0}{2}C + \frac{\tau_0^2}{4}PR\right) + \left(I - \frac{\tau_0}{2}C + \frac{\tau_0^2}{4}PR\right) \right\| \\
&= 2\tau_0 M \psi_{\min}^{-1} \left\| I + \frac{\tau_0^2}{4}PR \right\|.
\end{aligned}$$

By Lemma 3.2,

$$|\mathbf{s}^+| \leq 4\tau_0 M \psi_{\min}^{-1} < \frac{4M}{3} \min_i \{h_i h_{i-1}\} \min\{a^2, b^2\}.$$

It follows that

$$\mathbf{s}^+ \leq \frac{4M}{3} \min_i \{h_i h_{i-1}\} \min\{a^2, b^2\} \mathbf{x}.$$

By Lemma 3.5 the last term in \mathbf{s} is bounded above, namely,

$$\mathbf{s}^- = -\mathbf{x} + \frac{\tau_0}{2}C\mathbf{x} - \frac{\tau_0^2}{4}PR\mathbf{x} \leq -\mathbf{x}.$$

As a consequence,

$$\mathbf{v}_1 - \mathbf{x} \leq \left(\frac{4M}{3} \min_i \{h_i h_{i-1}\} \min\{a^2, b^2\} - 1 \right) \mathbf{x} \leq 0. \quad \square$$

The above proof can be easily modified to generate the following result.

Corollary 3.1. Let $\mathbf{g}(\mathbf{v}^0) = \mathbf{g}(\mathbf{v}_0)$ in Eq. (2.8). If

$$\frac{\tau_0}{\beta_{\min}} < \min\{a^2, b^2\}$$

and

$$\min_i \{h_i h_{i-1}\} < \frac{3}{2(\|\mathbf{v}_0\| + f(\|\mathbf{v}_0\|)) \min\{a^2, b^2\}}$$

then given $\mathbf{v}_0 < 1$ all the components of $\mathbf{v}_1 < 1$.

The following lemma shows that for a nonuniform time step the solution will monotonically increase prior to quenching provided τ_k is sufficiently small.

Lemma 3.7. Let all components of $\mathbf{v}_k < 1$ ($k \geq \ell$) and $C\mathbf{v}_\ell + \mathbf{g}(\mathbf{v}_\ell) > 0$, where $\ell \geq 0$ is a beginning time step. If $\frac{\tau_k}{\beta_{\min}} < \min\{a^2, b^2\}$ and τ_k is sufficiently small for all $k > \ell$, then $\mathbf{v}_{k+1} > \mathbf{v}_k$ for all $k > \ell$. That is, the sequence $\{\mathbf{v}_k\}_{k \geq \ell}$ is monotonically increasing before it quenches.

Proof. Consider the difference of \mathbf{v}_k after one time step

$$\begin{aligned}
\mathbf{v}_{k+1} - \mathbf{v}_k &= \left(I - \frac{\tau_k}{2}R\right)^{-1} \left(I - \frac{\tau_k}{2}P\right)^{-1} \left(I + \frac{\tau_k}{2}P\right) \left(I + \frac{\tau_k}{2}R\right) \left(\mathbf{v}_k + \frac{\tau_k}{2}\mathbf{g}(\mathbf{v}_k)\right) + \frac{\tau_k}{2}\mathbf{g}(\mathbf{v}_k) - \mathbf{v}_k + O(\tau_k^2) \\
&= \tau_k \left(I - \frac{\tau_k}{2}R\right)^{-1} \left(I - \frac{\tau_k}{2}P\right)^{-1} (C\mathbf{v}_k + \mathbf{g}(\mathbf{v}_k)) + O(\tau_k^2).
\end{aligned} \tag{3.1}$$

For $k = \ell$ it is assumed that $C\mathbf{v}_k + \mathbf{g}(\mathbf{v}_k) > 0$ then by Lemma 3.2 it is clear that $\mathbf{v}_{\ell+1} > \mathbf{v}_\ell$ provided τ_k is sufficiently small. For $k > \ell$ it can be shown by induction that $C\mathbf{v}_k + \mathbf{g}(\mathbf{v}_k) > 0$. We have

$$\begin{aligned} C\mathbf{v}_k + \mathbf{g}(\mathbf{v}_k) &= \mathbf{g}(\mathbf{v}_k) - \mathbf{g}(\mathbf{v}_{k-1}) + C\mathbf{v}_{k-1} + \mathbf{g}(\mathbf{v}_{k-1}) + C(\mathbf{v}_k - \mathbf{v}_{k-1}), \\ &= \left[\left(I - \frac{\tau_{k-1}}{2} P \right) \left(I - \frac{\tau_{k-1}}{2} R \right) + C\tau_{k-1} \right] \left(I - \frac{\tau_{k-1}}{2} R \right)^{-1} \left(I - \frac{\tau_{k-1}}{2} P \right)^{-1} (C\mathbf{v}_{k-1} + \mathbf{g}(\mathbf{v}_{k-1})) \\ &\quad + \mathbf{g}(\mathbf{v}_k) - \mathbf{g}(\mathbf{v}_{k-1}) + O(\tau_{k-1}^2) \\ &= \left(I + \frac{\tau_{k-1}}{2} C + \frac{\tau_{k-1}^2}{4} PR \right) \left(I - \frac{\tau_{k-1}}{2} R \right)^{-1} \left(I - \frac{\tau_{k-1}}{2} P \right)^{-1} (C\mathbf{v}_{k-1} + \mathbf{g}(\mathbf{v}_{k-1})) \\ &\quad + \mathbf{g}(\mathbf{v}_k) - \mathbf{g}(\mathbf{v}_{k-1}) + O(\tau_{k-1}^2) \\ &= \left(I + \frac{\tau_{k-1}}{2} P \right) \left(I + \frac{\tau_{k-1}}{2} R \right) \left(I - \frac{\tau_{k-1}}{2} R \right)^{-1} \left(I - \frac{\tau_{k-1}}{2} P \right)^{-1} (C\mathbf{v}_{k-1} + \mathbf{g}(\mathbf{v}_{k-1})) \\ &\quad + \mathbf{g}(\mathbf{v}_k) - \mathbf{g}(\mathbf{v}_{k-1}) + O(\tau_{k-1}^2). \end{aligned}$$

As a consequence, using Lemma 3.2 shows that $C\mathbf{v}_k + \mathbf{g}(\mathbf{v}_k) > 0$ for sufficiently small τ_{k-1} . It follows that for sufficiently small τ_k that $\mathbf{v}_{k+1} > \mathbf{v}_k$ which is the desired result. \square

The following theorem brings together the results from all the preceding lemmas.

Theorem 3.1. For any beginning time step ℓ , if

- (i) $\Delta x_i = \Delta y_i = h_i$ such that $\min_i \{h_i h_{i-1}\} < 3 / (2(\|\mathbf{v}_0\| + f(\|\mathbf{v}_0\|)) \min \{a^2, b^2\})$,
- (ii) $\frac{\tau_k}{\beta_{\min}} < \frac{1}{4} \min \{a^2, b^2\}$ for all $k \geq \ell$,
- (iii) Either
 1. (variable) $C\mathbf{v}_\ell + \mathbf{g}(\mathbf{v}_\ell) > 0$ and τ_k is sufficiently small,
 2. (uniform) $C\mathbf{v}_\ell + \mathbf{g}(\mathbf{v}_\ell) + \frac{\tau_\ell}{4} PR\mathbf{g}(\mathbf{v}_\ell) > 0$ and $\tau_k = \tau_\ell$ for all $k \geq \ell$,

then the sequence $\{\mathbf{v}_k\}_{k \geq \ell}$ produced by the adaptive Peaceman–Rachford splitting increases monotonically until unity is exceeded by a component of the solution vector or converges to the steady solution of the problem for both constant and variable τ_k , $k \geq \ell$.

4. Stability

Although the quenching type reaction–diffusion problem (1.1)–(1.3) and its discretizations including (2.2)–(2.4) are highly nonlinear, localized linear stability analysis, in which all underlying nonlinear terms are frozen, has proven to be an effective tool to evaluate the stability feature of the numerical methods derived for applications [5,10,11,21,7]. We also adopt this concept in our investigation.

Lemma 4.1. For any temporal step τ_k the infinity norm of the matrices

$$\left\| \left(I - \frac{\tau_k}{2} P \right)^{-1} \right\|, \left\| \left(I - \frac{\tau_k}{2} R \right)^{-1} \right\| \leq 1.$$

Proof. Consider $(I - \frac{\tau_k}{2} P)^{-1}$ and set

$$\alpha_j^{(i)} = 1 - \frac{\tau_k}{2} B_{jj}^{(i)} (m_j + (l_{j-1} + u_j)).$$

Since the matrix T is diagonally dominant and $\frac{\tau_k}{2} B_{jj}^{(i)} > 0$ then it is clear that $\alpha_j^{(i)} \geq 1$. The desired result is thus guaranteed by using the Varah-bound [26]. Similarly,

$$\beta_j^{(i)} = 1 - \frac{\tau_k}{2} B_{ii}^{(j)} (m_i + (l_{i-1} + u_i)) \geq 1$$

and as a consequence the infinite norm of $(I - \frac{\tau_k}{2} R)^{-1} \leq 1$. \square

Lemma 4.2. Let $\frac{\tau_k}{\beta_{\min}} < \min \{a^2, b^2\}$, then

$$\left\| \left(I + \frac{\tau_k}{2} P \right) \left(I + \frac{\tau_k}{2} R \right) \right\| = 1.$$

Proof. By Lemma 3.4, matrices $I + \frac{\tau_k}{2} P$ and $I + \frac{\tau_k}{2} R$ are nonnegative and therefore so is its product. It is clear from Lemma 3.5 that $\max \left\{ \left(I + \frac{\tau_k}{2} C + \frac{\tau_k^2}{4} PR \right) \mathbf{x} \right\} \leq 1$, where $\mathbf{x} = (1, \dots, 1)^\top$. In addition, hence the infinity norm is bounded by one.

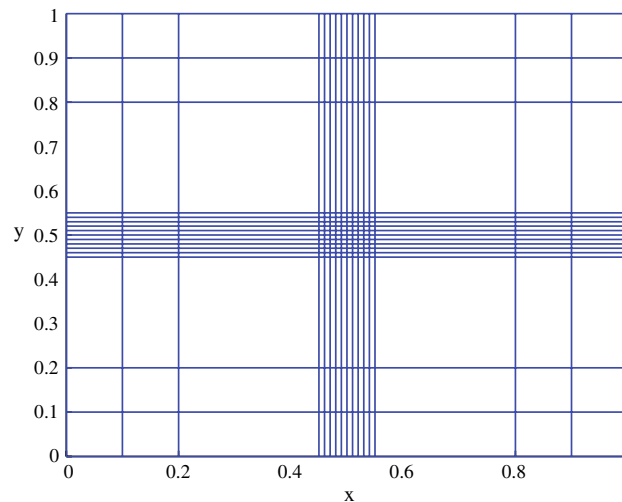


Fig. 2. The symmetric mesh given in Eq. (4.1).

Table 1

The computed norms of the involved matrices in the Peaceman–Rachford splitting method (2.8) using the mesh generated in Eq. (4.1).

	$(I - \frac{\tau}{2}R)^{-1}$	$(I - \frac{\tau}{2}P)^{-1}$	$(I - \frac{\tau}{2}R)^{-1} (I - \frac{\tau}{2}P)^{-1} (I + \frac{\tau}{2}P) (I + \frac{\tau}{2}R)$
$\ \cdot\ $	1.0000000000000000	1.0000000000000000	1.0000000000000000
$\ \cdot\ _2$	1.000641894664932	1.000641894664933	1.002578383099975

Equality is achieved by considering the non-positive matrix $\frac{\tau_k}{2}C + \frac{\tau_k^2}{4}PR$. For the prescribed τ_k , $(\frac{\tau_k}{2}C + \frac{\tau_k^2}{4}PR)\mathbf{x} \in (-1, 0]$.

Therefore $\max \left\{ \left(I + \frac{\tau_k}{2}C + \frac{\tau_k^2}{4}PR \right) \mathbf{x} \right\} = 1$. \square

The bound in Lemma 4.1 is sharp. Furthermore, the bound is sharp for part of the amplification matrix. It can be shown that equality is acquired or approached as the number of grid points tends to infinity. In the following example it is shown that for even a finite number of grid points a mesh can be constructed satisfying the criterion on τ for which the norm of the matrix operator generated by the Peaceman–Rachford splitting method can equal one to within machine precision.

Example 4.1. Let $h = 0.1$, $q = 0$, and $a = b = 1$. Choose $\tau = 10^{-6} < \frac{1}{3}10^{-4}$. Define

$$X_j = \begin{cases} jh & 0 \leq j \leq 2, \\ 0.45 + 0.1(j-3)h & 3 \leq j \leq 13, \\ 0.8 + (j-14)h & 14 \leq j \leq 16. \end{cases} \quad (4.1)$$

MATLAB[®] was used in calculating the matrices P and R and subsequent norms. In Table 1 the norms of $(I - \frac{\tau}{2}P)^{-1}$, $(I - \frac{\tau}{2}R)^{-1}$, and $(I - \frac{\tau}{2}P)^{-1} (I - \frac{\tau}{2}R)^{-1} (I + \frac{\tau}{2}P) (I + \frac{\tau}{2}R)$ are shown. The ℓ^2 -norm is also included for illustrative purposes. All quantities are evaluated using the desirable norm in double precision. The mesh generated by Eq. (4.1) is shown in Fig. 2.

Remark 4.1. That equality can be achieved should not be surprising as no restriction on the smoothness of the mesh has been enforced. However, it is worth noting that the above mesh is a realistic example for which one may wish to resolve fast changes in the gradient at $x = y = 0.5$. One should expect that strict equality could be enforced by further restricting the mesh, in particular enforcing smoothness conditions. It is clear that the current criterion on τ_k does not guarantee that the ℓ^2 -norm is less than or equal to one.

With the above example in mind, it is shown that the algorithm is weakly stable in the von Neumann sense with the nonlinear term frozen.

Theorem 4.1. Let $\frac{\tau_k}{\beta_{\min}} < \min \{a^2, b^2\}$. Then the Peaceman–Rachford splitting on symmetrically graded meshes (with the nonlinear term frozen) is weakly stable in the von Neumann sense.

Proof. Consider a perturbation at time step k of $\mathbf{z}_k = \mathbf{v}_k - \tilde{\mathbf{v}}_k$, where $\tilde{\mathbf{v}}_k$ is the computed solution. By Lemmas 4.1 and 4.2 the norm is bounded,

$$\begin{aligned}\|\mathbf{z}_{k+1}\| &= \left\| \left(I - \frac{\tau_k}{2}R\right)^{-1} \left(I - \frac{\tau_k}{2}P\right)^{-1} \left(I + \frac{\tau_k}{2}P\right) \left(I + \frac{\tau_k}{2}R\right) \mathbf{z}_k \right\| \\ &\leq \left\| \left(I - \frac{\tau_k}{2}R\right)^{-1} \right\| \left\| \left(I - \frac{\tau_k}{2}P\right)^{-1} \right\| \left\| \left(I + \frac{\tau_k}{2}P\right) \left(I + \frac{\tau_k}{2}R\right) \right\| \|\mathbf{z}_k\| \leq \|\mathbf{z}_k\|.\end{aligned}\quad (4.2)$$

The above ensures the theorem. \square

Remark 4.2. This is an improvement over the conclusion in Theorem 4.1 of [10]. This is owed to the tighter bounds on the norm of the involved matrices in Lemmas 4.1 and 4.2.

More importantly an initial perturbation can be bounded in the infinity norm, for which is stated concisely in the following theorem.

Theorem 4.2. Let $\frac{\tau_i}{\beta_{\min}} < \min\{a^2, b^2\}$ for all $i \leq k$. Then the linearized variable step Peaceman–Rachford method on symmetrically graded meshes (with the nonlinear term frozen) is weakly stable in the von Neumann sense under the l_∞ norm, i.e.,

$$\|\mathbf{z}_{k+1}\| \leq \|\mathbf{z}_0\|,$$

where $\mathbf{z}_0 = \mathbf{v}_0 - \tilde{\mathbf{v}}_0$ is an initial perturbation or error. $\mathbf{z}_{k+1} = \mathbf{v}_{k+1} - \tilde{\mathbf{v}}_{k+1}$ is the perturbation arising from the initial perturbation \mathbf{z}_0 .

Proof. The proof can be acquired conveniently from repeated use of Theorem 4.1. \square

5. Numerical experiments

We present two typical numerical experiments illustrating the feasibility in calculating the quenching time for two-dimensional reaction–diffusion equations of the form

$$\begin{aligned}(x^2 + y^2)^{q/2} u_t &= u_{xx} + u_{yy} + \frac{1}{1-u}, \quad 0 \leq q < 2, (x, y, t) \in \Omega, \\ u(x, y, t) &= 0, \quad (x, y, t) \in S, \\ u(x, y, 0) &= u_0(x, y), \quad (x, y) \in D.\end{aligned}$$

In each example we employ a standard Peaceman–Rachford splitting method together with a temporal adaptation (2.9). A nonuniform exponentially graded mesh centered around the ideal quenching point [14,5], X^* , is used in the calculation with a resolution of $\delta = 10^{-4}$ near the quenching point, namely,

$$X_j = \begin{cases} X^* \left(1 - \left(\frac{\delta}{X^*}\right)^{\frac{j}{N^*-1}}\right) & 0 \leq j \leq N^* - 1, \\ X^* & j = N^*, \\ X^* + (1 - X^*) \left(\frac{\delta}{1 - X^*}\right)^{\frac{2N^*-j}{N^*-1}} & N^* + 1 \leq j \leq 2N^*, \end{cases} \quad (5.1)$$

where $N^* = \frac{1}{2}(N - 1)$ and N is the number of grid points. In general X^* is not known but an approximation can be found numerically [5,22]. In the cases considered the quenching point occurs along the line $y = x$, in particular at $X^* = 0.5$ for $q = 0$. In such a case, as an illustration, the mesh generated by Eq. (5.1) is shown in Fig. 3.

Remark 5.1. An adaptation of the grid could be considered using a modified arc-length adaptive principal. This can be accomplished through monitoring the arc-length of the line $u_t(x, x, t)$, more precisely,

$$\int_{x_j}^{x_{j+1}} \sqrt{1 + u_{tx}(x, x, t)} dx = \frac{1}{M} \int_0^1 \sqrt{1 + u_{tx}(x, x, t)} dx, \quad 0 \leq j \leq M,$$

where $M + 1$ is the number of grid points. It is clear that as the discrete solution approaches the quenching time the mesh adaptation is hindered by the unbounded growth in the arc-length of $u_t(x, x, t)$. An artificial remedy is to impose an upper and lower bound on the mesh size for which the adaptation ceases the first time a particular h_i is outside of the proposed interval. The algorithm would then proceed with the fixed mesh till the quenching time is calculated.

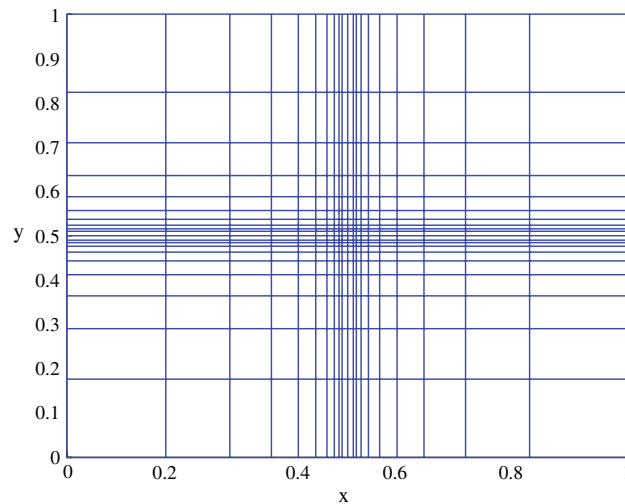


Fig. 3. The exponentially graded mesh for $X^* = 1/2$, $\delta = 10^{-2}$, and $N = 21$.

Table 2

A comparison of the calculated quenching domains D_{new} using the exponentially graded mesh ($N = 21$) versus known theoretical (D_C) and numerical (D_S), (D_L) results. The quenching times for D_S and D_L are taken from [10, 7]. The quenching time for D_{new} is calculated with the algorithm proposed in this paper. Numerical quenching is not observed for $D = D_C$ with the employed method in this paper. Parameters $q = 0$, $\theta = 1$, $a/b = 1$.

Domain size	Quenching time
4.960600 (D_S)	5.72475
4.453978 (D_L)	548.99485
4.453855 (D_{new})	71.80331
4.45375 (D_C)	N/A

The initial time step is chosen to satisfy the criterion provided in Theorems 3.1, 4.1 and 4.2. The minimum time step is set at 10^{-10} . The exponential graded mesh in Eq. (5.1) is used for $N = 21$. This will generate matrices of a moderate size 361×361 . The initial condition is set to zero. The quenching time is determined as the time step for which at the next iteration the solution first surpasses or equals to one.

Example 5.1. Let $q = 0$. In [5] there was an apparent difference in the calculated quenching domains versus known theoretical work in the case of $a = b = 1$ [17,18,6]. The quenching domain was then further resolved in [10]. Again, the quenching domain is calculated here using the adaptive Peaceman–Rachford splitting method and the exponential grid with $N = 21$ and $\delta = 10^{-2}$.

The grid resolution near the known quenching point, $(1/2, 1/2)$, is of order 10^{-2} . As a comparison to using a uniform mesh one would need $O(10^2)$ points to obtain a similar resolution. In that case, the matrices would be of $O(10^4) \times O(10^4)$ making the required inversion in the adaptive Peaceman–Rachford formula (2.8) much more costly and time-prohibitive.

The quenching domain is calculated by creating a sequence of domains for which quenching occurs. The size of each domain is reduced iteratively till numerical quenching is not observed. The quenching domain is then calculated as the smallest, observed domain for which numerical quenching did occur. Table 2 provides a comparison of our calculated quenching domain (D_{new}) for the case of $a/b = 1$ to previous theoretical [18,3] (D_C) and numerical [5,10] (D_S , D_L) results, respectively. The first column lists the calculated quenching domains followed by their respective quenching times in the adjacent column. The solution and its time derivative just prior to the onset of quenching is shown in Fig. 4.

Example 5.2. Let $q = 1$. In this case the degeneracy term in Eq. (1.1) will affect the location of the quenching point [5,3,21]. We again employ our method in the calculating the quenching domain for the typical case of $a = b = 1$. It has been observed that the quenching point will shift toward the origin as a result of the degeneracy at the origin [10,7]. The quenching domain is given in Table 3 with its corresponding quenching time.

The reduction in the quenching domain is a result of the degeneracy. However, it is interesting that the domain is only reduced slightly by roughly 1.55×10^{-4} although the equations themselves are more singular in nature. The quenching point's location is $(0.490, 0.490)$ or $(1.034, 1.034)$ in the scaled and unscaled variables, respectively.

In Fig. 6 we give multiple plots of the derivative graph with its corresponding numerical solution just prior to quenching. As the quenching time approaches the gradient of $u(x, y, t)$ changes quite rapidly in the vicinity of the quenching location. Hence it is desirable to have a resolved mesh near that location. As expected, the change in u_t is extremely fast. In particular, from Fig. 6(a) to (d) there is only a change of approximately 2×10^{-6} in time, but u_t has changed by two orders of magnitude.

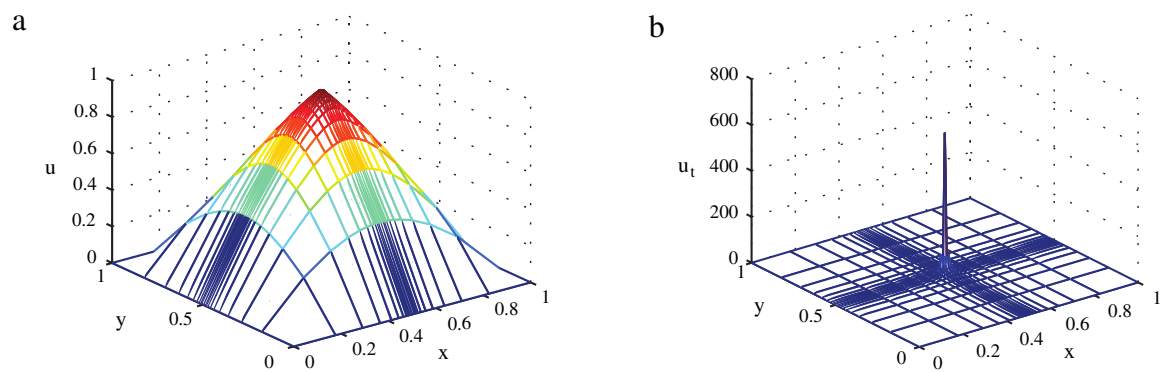


Fig. 4. (a) The solution u and (b) the derivative function u_t at $t = 71.80331$ just prior to quenching in the scaled variables. The maximum value of u_t is 608.6337. Quenching occurs at $(1/2, 1/2)$. Parameters $q = 0, \theta = 1, a/b = 1, D = 4.453855$.

Table 3
The calculated quenching domain, time, and location (scaled variables) using the exponentially graded mesh ($N = 21$). A cluster of 16 points located near the origin with equal spacing of .01 is added as a precaution to resolve the effect of the degeneracy. Parameters $q = 1, \theta = 1, a/b = 1$ are used.

Domain size	Quenching time	Quenching location
4.45370	18.4982474	(0.490, 0.490)

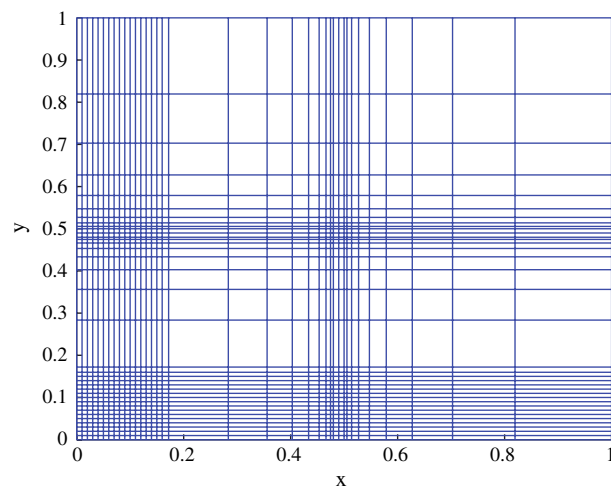


Fig. 5. The exponentially graded mesh ($N = 21$) with a cluster of points with a .01 spacing was used in the computations for $q = 1$. A total number of 1225 interior grid points are considered.

Remark 5.2. The relative few points used in the above examples is a direct result of using a non-uniform grid that was created based on a good approximation to the quenching point, (X^*, X^*) . A sufficiently close approximation to X^* is necessary when using a minimal number of grid points. Again, the choice of X^* can be done numerically, but another approach is to search for the maximum value of u_t 's location and then let X^* be the x -coordinate of that location. The mesh can then be updated accordingly and the new solution vector can be constructed using standard interpolators.

Remark 5.3. This example indicates the advantage of using a priori knowledge to construct exponential grids. As the strength of the degeneracy increases, it will become imperative to employ spatial adaption to track the movement of the quenching location. Here, only $q = 1$ has been given as the analysis of the algorithm that employs spatial adaption is not complete and is a current area of research.

6. Conclusions

In this paper an adaptive Peaceman–Rachford splitting method is developed for solving quenching-type problems in the form of degenerate reaction–diffusion equations which are discretized over nonuniform grids. A condition on the maximum

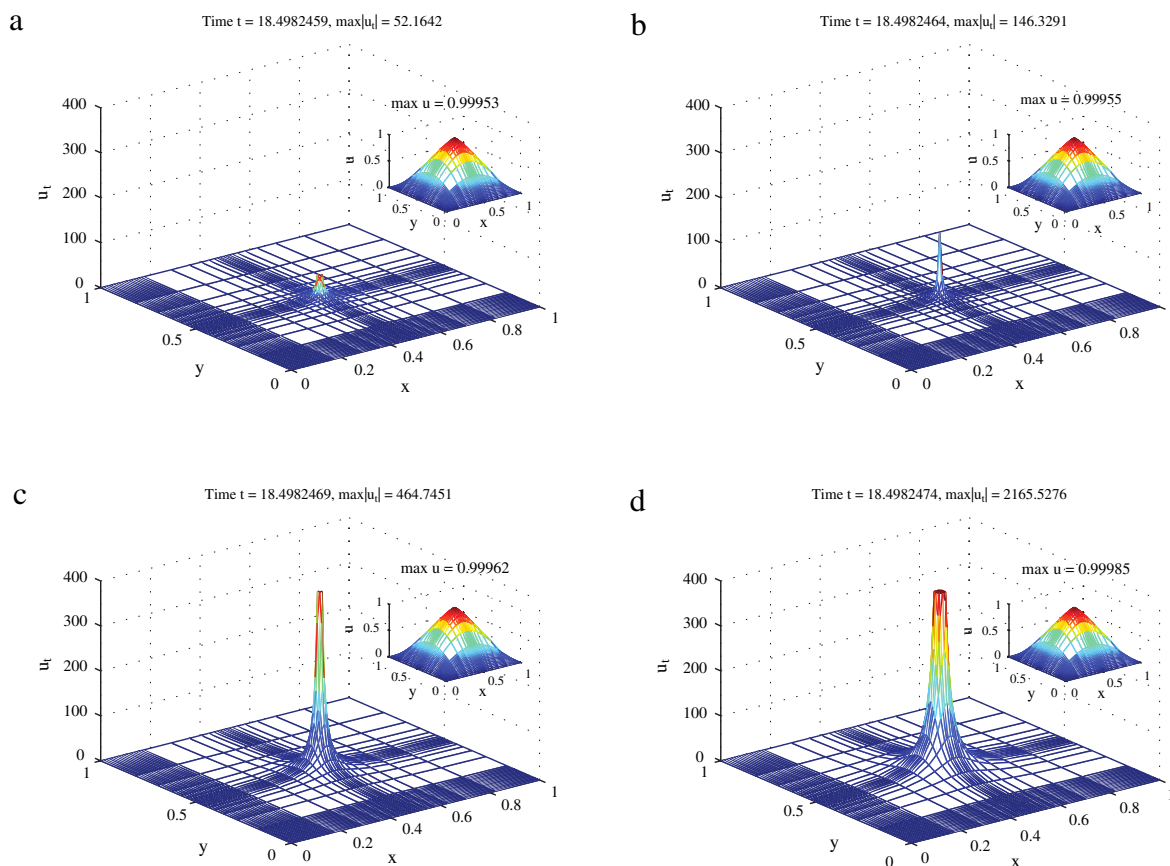


Fig. 6. Multiple plots of the derivative function u_t paired with u as it evolves. (a) $t = 18.4982459$, (b) $t = 18.4982464$, (c) $t = 18.4982469$, and (d) $t = 18.4982474$. The fast change in the time-derivative motivates the need to resolve the grid closely at the quenching location and adaptively choose the time step. The exponentially grade mesh for $N = 21$ with a cluster of points close to the degeneracy is used (see Fig. 5). The axes are held fixed. Peak values of u_t are removed in (c) and (d) to see more details of the blow-up structures. Parameters $q = 1$, $\theta = 1$, $a/b = 1$, $D = 4.45370$.

step-size is derived to ensure the positivity and monotonic property in the numerical solution. The condition acquired is related to the minimum spatial step-size in addition to the maximum value of the degenerate function. It is shown that the maximum temporal step is greatly reduced for larger values of q close to two. That is to be expected as the singularity introduced by the degeneracy will need to be resolved at extremely fine time steps. In such situations, it is suggested that adaptation in the spatial grids is necessary, hence is an active area of future exploration.

To guarantee the monotonicity of the discrete solution in the underlying nonuniform mesh situation, the time step restriction is a third lower than that known for the uniform case [21,7]. It is anticipated that with appropriate bounds on the smoothness of the mesh that the reduction can be lifted. Without further restrictions it has been observed that one can easily create nonuniform meshes that the amplification matrix's norm will equal to one and, moreover, be greater than the unity in the ℓ^2 -norm. Even so, one can prove that the corresponding eigenvalues are still within the interval $(-1, 0)$. It seems evident there is a need to explore this issue further. It is the authors' belief that this will further complicate the grid adaptation as the mesh will need to adhere to the smoothness criterion set forth by the analysis rather than evolving according to the physics portrayed in numerical computations. Regardless, weak stability is still guaranteed in the von Neumann sense for the ∞ -norm and computational experiments indicate good agreement with known theoretical and experimental results via fairly coarse grids.

Acknowledgments

We would like to thank the anonymous referees for their time and comments. Incorporating their suggestions has greatly enhanced the quality and presentation of this paper.

References

- [1] A. Acker, B. Kawohl, Remarks on quenching, *J. Nonlinear Anal.* 13 (1) (1989) 53–61.
- [2] T. Boni, Extinction for discretizations of some semilinear parabolic equations, *Acad. Sci. Paris. Sér. I Math.* 8 (2001) 795–800.

- [3] N. Nouaili, A Liouville theorem for a heat equation and applications for quenching, *Nonlinearity* 24 (2011) 797–832.
- [4] Q. Sheng, A. Khaliq, A compound adaptive approach to degenerate nonlinear quenching problems, *Numer. Methods Partial Differential Equations* 15 (1999) 29–47.
- [5] H. Cheng, P. Lin, Q. Sheng, R. Tan, Solving degenerate reaction–diffusion equations via variable step Peaceman–Rachford splitting, *SIAM J. Sci. Comput.* 25 (2003) 1273–1292.
- [6] C. Kirk, W. Olmstead, Blow-up in a reactive–diffusive medium with a moving heat source, *J. Zeitschrift Angew. Math. Phys.* 53 (2002) 147–159.
- [7] Q. Sheng, A. Khaliq, *Adaptive Method of Lines*, CRC Press, London, New York, 2001 (Chapter 9).
- [8] P. Ferreira, Numerical quenching for the semilinear heat equation with a singular absorption, *J. Comput. Appl. Math.* 228 (2009) 92–103.
- [9] H. Levine, Quenching, nonquenching, and beyond quenching for solutions of some parabolic equations, *Ann. Math. Pure Appl.* 4 (1989) 243–260.
- [10] K. Liang, P. Lin, M. Ong, R. Tan, A splitting moving mesh method for reaction–diffusion equations of quenching type, *J. Comput. Phys.* 215 (2006) 757–777.
- [11] J. Mooney, A numerical method for accurate critical length estimation in singular quenching problems, *World Sci. Ser. Appl. Anal.* 4 (1995) 505–516.
- [12] F. N’Gohisse, T. Boni, Quenching time of some nonlinear wave equations, *Arch. Math.* 45 (2009) 115–124.
- [13] W. Wang, S. Zheng, Asymptotic estimates to quenching solutions of heat equations with weighted absorptions, *Asymp. Anal.* 70 (2010) 125–139.
- [14] J. Bebernes, D. Eberly, *Mathematical Problems from Combustion Theory*, Vol. 83, Springer-Verlag, 1989, pp. 7–9.
- [15] M. Floater, Blow-up at the boundary for degenerate semilinear parabolic equations, *Arch. Ration. Mech. Anal.* 114 (1991) 57–77.
- [16] H. Ockendon, Channel flow with temperature-dependent viscosity and internal viscous dissipation, *J. Fluid Mech.* 93 (1979) 737–746.
- [17] T. Boni, On quenching of solution for some semilinear parabolic equation of second order, *Bull. Belg. Math. Soc.* 5 (2000) 73–95.
- [18] C. Chan, L. Ke, Parabolic quenching for nonsmooth convex domains, *J. Math. Anal. Appl.* 186 (1994) 52–65.
- [19] R. Furzeland, J. Verwer, P. Zegeling, A numerical study of three moving-grid methods for one-dimensional partial differential equations which are based on the method of lines, *J. Comput. Phys.* 89 (1990) 349–388.
- [20] J. Lang, A. Walter, An adaptive rothe method for nonlinear reaction–diffusion systems, *Appl. Numer. Math.* 13 (1993) 135–146.
- [21] Q. Sheng, Adaptive decomposition finite difference methods for solving singular problems, *Frontiers Math. China* 4 (2009) 599–626.
- [22] Q. Sheng, H. Cheng, An adaptive grid method for degenerate semilinear quenching problems, *Computers Math. Appl.* 39 (2000) 57–71.
- [23] S. Chin, A fundamental theorem on the structure of symplectic integrators, *Phys. Lett. A* 354 (2006) 373–376.
- [24] B. Jain, A. Sheng, An exploration of the approximation of derivative functions via finite differences, *Rose–Hulman Undergrad. Math. J.* 8 (2007) 172–188.
- [25] P. Henrici, *Discrete Variable Methods in Ordinary Differential Equations*, John Wiley & Sons, Inc., New York, 1962, pp. 360–365.
- [26] J. Varah, A lower bound for the smallest singular value of a matrix, *Linear Algebra Appl.* 11 (1975) 3–5.